Numerical Analysis of Convection in the Inner Core (DRAFT)

Maximilian Williams

September 2021

Abstract

Convection in the Earth's inner core has been a contentious topic in geoscience. Recently, it has been proposed through siesmic observations that Earths inner core is convecting. Here we numerically model convection in the Inner core, using the streamfunction-vorticity formulation and lattice boltzman method in 2-dimensions.

Introduction

In this report, we use two vastly different numerical tehcniques, the vorticity-streamfunction method and the Thermal Lattice Boltzman Method to simulate convection in an internally heated, self-gravitating bousiniesque fluid. Two codes are produced in python using the streamfunction-vorticity formulation in cartesian and polar coordinates. A single Thermal Lattice Boltzman Method (TLBM) code is produced in goLang. The python codes use limited libraries such as numpy while the goLang code uses only inbuilt libraries math, random numbers etc...

Plan: I want to also talk about why this is actually important, why is this something that is worth studying
Here I want to introduce the physics of what I want to talk about. I want to introduce the basic equations that I will use.

Governing Equations

In this section I introduce the physics of the problem; the governing equations that we wish to numerically solve.

Throughout analysis we describe the fluid in the Eularian frame under a graviational acceleration $\vec{g}$ which may vary in space. We give each location in the fluid a velocity $\vec{u}$ and density ρ that vary in space $\vec{x}$ and time t. We assume the fluids viscosity μ, thermal diffusivity κ and specific heat capacity C_p are all constants. By conserving fluid momentum, we produce the navier stokes equation:

$$\rho\frac{D\vec{u}}{Dt} = \rho\vec{g} - \nabla p + \mu\nabla^2\vec{u}, \tag{1}$$

where $\frac{D}{Dt} = \frac{\partial}{\partial t} + (\vec{u} \cdot \nabla)$ is the material derivative, p the pressure of the fluid and ∇ the del operator. The dynamics of fluid temperature T are described the inhomoenous advection diffusion equation:

$$\frac{DT}{Dt} = \kappa\nabla^2 T + \frac{Q}{C_v\rho}, \tag{2}$$

where Q is the heat generated per unit volume per unit time, C_v the specific heat at constant volume and ρ the fluid density. The density of the fluid ρ is assumed to vary linearly in temeprature according to the equation of state:

$$\rho = \rho_0(1 - \alpha(T - T_0)), \tag{3}$$

where α is the volumetric expansion coeffecient and ρ_0 the density at a reference temperature T_0. Through siesmic imaging, variations in inner core density are $<< 1\%$. We also assume that the inner cores evolution occures over geologic timescales, and as such take $\vec{u}$ to be first order. These assumptions allow us to make the slow flow boussinesq approximation to equation 1:

$$\frac{\partial\vec{u}}{\partial t} = \frac{\rho'}{\rho}\vec{g} - \frac{\nabla p'}{\rho_0} + \nu\nabla^2\vec{u}, \tag{4}$$

where $\rho' = -\alpha(T - T_0)$, ν the kinomatic viscosity $\nu = \frac{\mu}{\rho_0}$ and p' a first order pertibation to the background pressure p_0.
The Earths

Numerical Methods

Two numerical methods are introduced for solving the thermal convection problem, the Lattice Boltzman Method and the streamfunction-vorticity formulation.

Streamfunction-Vorticity formulation

Here I introduce the streamfunction-vorticity method for use in 2 dimensions and use it to eliminate pressure terms in 4 and 2 in cartesian and polar geometries giving a set of numerically solvable equations.

The streamfunction-vorticity formulation is a popular method for analytical and simple numerical analysis of incompressable fluids in two dimensions. Its main advantage is its elimination of all pressure terms, which would typically require iterative techniques to solve, as is used in the SIMPLE algorithm. However, the streamfunction-vorticity method is limited to 2-dimensional or 3-dimensional symmetric flows and so has limited applicability.

We define two scalar quantities, the vorticity ω and the streamfunction ψ. The vorticity ω is given by:

$$\omega = (\nabla \times \vec{u})_z, \tag{5}$$

where the z subscript denotes the component out of the plane. We also define a streamfunction ψ by:

$$\omega = -\nabla^2 \psi. \tag{6}$$

Given a coordinate system, and a clever definition of $\vec{u}$ we can rewrite equations 2 and 4 in terms of ω and ψ rather than $\vec{u}$ and p. In cartesian coordinates (x, y) we pick

$$u = \frac{\partial \psi}{\partial y}, v = -\frac{\partial \psi}{\partial x}, \tag{7}$$

allowing us to write equations 2 and 4 as:

$$\frac{\partial T}{\partial t} + \frac{\partial \psi}{\partial y}\frac{\partial T}{\partial x} - \frac{\partial \psi}{\partial x}\frac{\partial T}{\partial y} = \kappa \nabla^2 T + \frac{Q}{\rho_0 C_v} \tag{8}$$

$$\frac{\partial w}{\partial t} = -\frac{g_y}{\rho_0}\frac{\partial \rho'}{\partial x} + \nu \nabla^2 \omega \tag{9}$$

Similary, in polar coordinates (r, θ) we pick:

$$u = \frac{1}{r}\frac{\partial \psi}{\partial \theta}, v = -\frac{\partial \psi}{\partial r}, \tag{10}$$

giving:

$$\frac{\partial T}{\partial t} + \frac{1}{r}\frac{\partial \psi}{\partial \theta}\frac{\partial T}{\partial r} - \frac{1}{r}\frac{\partial \psi}{\partial r}\frac{\partial T}{\partial \theta} = \kappa \nabla^2 T + \frac{Q}{\rho_0 C_v} \tag{11}$$

and,

$$\frac{\partial \omega}{\partial t} = -\frac{g_r}{\rho_0 r}\frac{\partial \rho'}{\partial \theta} + \nu \nabla^2 \omega. \tag{12}$$

A full derivation of equations 8, 9, 11, 12 are given in appendix. Importantly, our definitions of u and v in equations 7 and 10 satisify equation 5 and 6. Equations 6, 8, 9 for the cartesian case and 6, 11, 12 for the polar case can be directly solved.

Solving the streamfunction-vorticity equations

The finite difference method used for solving the streamfunction-vorticity-formulated governing equations is shown

We first discritize our domain $\mathcal{D}$. In the cartesian case, we use $(x_i, y_j) = (i\Delta x, j\Delta y)$ with integers i and j satisfying $0 \leq i < N_x$ $0 \leq j < N_y$. In the polar case, we use $(r_i, \theta_j) = (R_0 + i\Delta r, j\Delta\theta)$ again with $0 \leq i < N_r$ and $0 \leq j < N_\theta$. We impose $\Delta\theta = \frac{2\pi}{N_\theta - 1}$ for consistancy with θ-periodic boundary conditions and an inner radius R_0 in polar coordinates to avoid singularities generated by $r = 0$. We also discritize time t by $t_n = n\Delta t$. For a function f, we use $f_{i,j}^n$ to mean f evaluated at time n at position (x_i, y_j) in cartesian coorindates or (r_i, θ_j) in polar coordinates.

To approximate derivatives we use a finite difference approach. All time derivatives are approximated by forward difference:

$$\frac{\partial f}{\partial t} = \frac{f^{n+1} - f^n}{\Delta t} \tag{13}$$

Second order space derivatives are apprimxated by a central difference:

$$\frac{\partial^2 f_{i,j}}{\partial x_1^2} = \frac{f_{i+1,j} - 2f_{i,j} + f_{i-1,j}}{\Delta x_1^2}, \tag{14}$$

$$\frac{\partial^2 f_{i,j}}{\partial x_2^2} = \frac{f_{i,j+1} - 2f_{i,j} + f_{i,j-1}}{\Delta x_2^2}, \tag{15}$$

where x_1 is the first coordinate and x_2 is the second coordinate. For example, in cartesian coordinates (x, y), we would have $x_1 = x$ and $x_2 = y$. For non advection terms, we approximate first order spatial derivaitves by:

$$\frac{\partial f_{i,j}}{\partial x_1} = \frac{f_{i+1,j} - f_{i-1,j}}{2\Delta x_1}, \tag{16}$$

2

and

$$\frac{\partial f_{i,j}}{\partial x_2} = \frac{f_{i,j+1} - f_{i,j+1}}{2\Delta x_2}.$$ (17)

For advection terms, of the form $a\frac{\partial f_{i,j}}{\partial x_1}$ we employ a first order godanov scheme:

$$a\frac{\partial f_{i,j}}{\partial x_1} = \frac{1}{\Delta x}(\mid a \mid (\frac{1}{2}f_{i+1,j} - \frac{1}{2}f_{i-1,j}) - a(\frac{1}{2}f_{i+1,j} - f_{i,j} - \frac{1}{2}f_{i-1,j})).$$ (18)

This scheme is always downstream, regardless of the direction of the advecting field a.

Other more accurate, but substantually more complex methods for solving these equations, particularlly the advection equation exists such as the semi-lagrange crank-nicolson scheme.

To solve the streamfuntion-vorticity equations we assume a starting vorticity ω on our domain $\mathcal{D}$. We then apply the Jacobi method to solve equation 6 for ψ on the interior of the domain which we call $\mathcal{D}'$. Using ψ we update T on $\mathcal{D}'$ using equation 8 (or 11 for polar). Finally, ω is updated on $\mathcal{D}'$ using equation 9 (12 for polar). This process is repeated.

The Jacobi Method

Here a basic numerical method for solving the Poisson equation, the Jacobi method is outlined. We cannot solve for ψ explicitly in equation 6. Instead we use an iterative jacobi method. In cartesian coordinates, equation 6 is:

$$\omega_{i,j} = \frac{\psi_{i+1,j} - 2\psi_{i,j} + \psi_{i-1,j}}{\Delta x^2} + \frac{\psi_{i,j+1} - 2\psi_{i,j} + \psi_{i,j-1}}{\Delta y^2}$$ (19)

Rearanging for ψ

$$\psi_{i,j} = \frac{\Delta x^2 \Delta y^2}{2(\Delta x^2 + \Delta y^2)}(\frac{\psi_{i+1,j} + \psi_{i-1,j}}{\Delta x^2} + \frac{\psi_{i,j+1} + \psi_{i,j-1}}{\Delta y^2} + \omega_{i,j}).$$ (20)

We then use the result of $\psi_{i,j}$ back into equation 20 to solve for $\psi_{i,j}$ iterately as shown in equation 21:

$$\psi_{i,j}^{(k+1)} = \frac{\Delta x^2 \Delta y^2}{2(\Delta x^2 + \Delta y^2)}(\frac{\psi_{i+1,j}^{(k)} + \psi_{i-1,j}^{(k)}}{\Delta x^2} + \frac{\psi_{i,j+1}^{(k)} + \psi_{i,j-1}^{(k)}}{\Delta y^2} + \omega_{i,j}).$$ (21)

Where the superscript (k) means the result of the kth iteration of the above equation and this operation us applied to all points in $\mathcal{D}'$. We terminate this iterative method once the error $\sum_{(i,j)\in\mathcal{D}'} \mid \psi_{i,j}^{(k+1)} - \psi_{i,j}^{(k)} \mid$ gets suffeciently small. A similar method is applied to the polar coordinate case.

Solution Stability and Accuracy

Lattice Boltzman Method

In this section I give a brief introduction to the Lattice Boltzman Method and why its different from most numerical tehcniques. I introduce a 2-dimensional lattice D2Q9 and discribe the Thermal Lattice Boltzman method (TLBM) which is employed by my numerical solution to simulate convection.

The Lattice Boltzman Method (LBM) is a generalization of a Lattice Gas Automata (LGA), which are themselves a specialized Automata for simulating fluid flows. These Automata methods like common fluid simulation techniques discritize space and time. They directly simulate the state of particles or their distributions and evolve in time accoring to rules which give the desired macroscopic fluid properties as an emergent effect. This is fundamentally different from typical approaches which amount to directly numerically solving a set of partial differential equations.

To discritize space, we place nodes at locations $(x_i, y_j) = (i, j)$ with i, j integers. Each node has attached to it a latitce, here the D2Q9 lattice shown in figure 1. The lattice defines unit vectors $\vec{e}_i$, $i \in \{0, 1, 2, 3, 4, 5, 6, 7, 8\}$. In addition, each direction e_i gets a weight w_i. In the D2Q9 lattice these are:

$$w_i = \begin{cases} \frac{4}{9} & \text{if } i = 0 \\ \frac{1}{9} & \text{if } i = 1, 2, 3, 4 \\ \frac{1}{36} & \text{if } i = 5, 6, 7, 8 \end{cases}.$$

We wish to simulate convection. For this, we require the particle motion and the internal energy throughout the lattice. We define two distribution functions $f_\alpha(\vec{x}, t)$ and $g_\alpha(\vec{x}, t)$ denoting the particle and internal energy distributions along direction α at lattice points $\vec{x}$ and times t. The direction can be thought of as the direction of flow for particles or energy. Each timestep there are two steps to updating f and g, a common streaming step:

$$f_\alpha(\vec{x} + \vec{e}_\alpha, t + \Delta t) = f_\alpha(\vec{x}, t),$$ (22)

and different collision steps:

$$f_\alpha(\vec{x} + \vec{e}_\alpha, t + \Delta t) = f_\alpha(\vec{x}, t) + \frac{1}{\tau_f}(f_\alpha^{eq}(\vec{x}, t) - f_\alpha(\vec{x}, t)) + F_\alpha$$ (23)
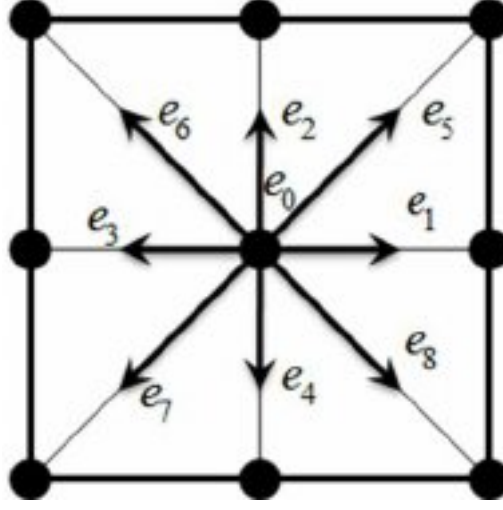
3

Figure 1: D2Q9 Lattice. Black notes repressent lattice points, vectors $e_0, .., e_8$ are the lattice vectors. Image sourced from [2]

$$g_\alpha(\vec{x} + \vec{e}_\alpha, t + \Delta t) = g_\alpha(\vec{x}, t) + \frac{1}{\tau_g}(g_\alpha^{eq}(\vec{x}, t) - g_\alpha(\vec{x}, t)) + G_\alpha. \tag{24}$$

Here F_α and G_α are the forcing terms terms and f_α^{eq} and g_α^{eq} are equilibrium distributions. The relaxation times τ_f and τ_g are related to the macroscopic thermal diffusivity (κ) and kinematic viscousity ν by:

$$\tau_g = \frac{3\kappa}{S^2 \Delta t} + \frac{1}{2} \tag{25}$$

and,

$$\tau_f = \frac{3\nu}{S^2 \Delta t} + \frac{1}{2}. \tag{26}$$

The equilibrium distributions are given by the BKG approximation:

$$f_\alpha^{eq}(\vec{x}, t) = \rho w_\alpha (1 + 3\frac{\vec{e}_\alpha \cdot \vec{u}}{s^2} + \frac{9}{2}\frac{(\vec{e}_\alpha \cdot \vec{u})^2}{c^4} - \frac{3}{2}\frac{\vec{u} \cdot \vec{u}}{c^2}), \tag{27}$$

$$g_\alpha^{eq}(\vec{x}, t) = \epsilon \rho w_\alpha (1 + 3\frac{\vec{e}_\alpha \cdot \vec{u}}{s^2} + \frac{9}{2}\frac{(\vec{e}_\alpha \cdot \vec{u})^2}{c^4} - \frac{3}{2}\frac{\vec{u} \cdot \vec{u}}{c^2}), \tag{28}$$

Here ρ, ϵ and $\vec{u}$ are the macroscopic density, internal energy and velocity given by:

$$\rho = \sum_{i=0}^{8} f_i, \tag{29}$$

$$\rho \vec{u} = \sum_{i=0}^{i=8} f_i \vec{e}_i \tag{30}$$

and,

$$\rho \epsilon = \sum_{i=0}^{i=8} g_i. \tag{31}$$

The forcing terms F_i and G_i are problem dependent. For thermal convection $G_i = 0$ and F_i is a gravitational term Δf_α:

$$\Delta f_\alpha = -w_\alpha \rho \alpha \epsilon \frac{\vec{e}_\alpha}{|\vec{e}_\alpha|} \cdot \vec{g} \frac{1}{\tau_{grav}}, \tag{32}$$

where $||$ is the vector norm and $\vec{g}$ is the gravitational acceleration. Here τ_{grav} is the relaxation time for the gravitational field. We take $\tau_g = 0.6$ here, following [3]. The algorithm used to evolve the above TLBM equations is given in algorithm 1

Boundary Conditions

In both streamfunction-vorticity codes, boundaries were assumed to be fluid-impermiable, non-slip and insulating. In the Lattice Boltzman code, "bounce back" boundary condition was used. This is a fluid-impermiable, insulating and slip boundry.

Algorithm 1 Thermal Lattice Boltzman Algorithm

$f_\alpha = \rho_0 w_\alpha$
$\epsilon = 0$
ϵ_b
$\rho = 0$
$\vec{u} = 0$
while Simulation Running **do**
    $g_\alpha + = \rho \epsilon_b w_\alpha$
    if $x - \vec{e}_\alpha$ is solid **then**
        $f_\alpha(x) = f_{\alpha'}(x)$
        $g_\alpha(x) = g_{\alpha'}(x)$
    else
        $f_\alpha(x) = f_\alpha(x - \vec{e}_\alpha)$
        $g_\alpha(x) = g_\alpha(x - \vec{e}_\alpha)$
    end if
    $\rho = \sum_{i=0}^{i=8} f_i$
    $\vec{u} = \frac{(\sum_{i=0}^{i=8} f_i \vec{e}_i)}{\rho}$
    $\epsilon = \frac{\sum_{i=0}^{i=8} g_i}{\rho}$
    $f_\alpha^{eq} = \rho w_\alpha (1 + 3\frac{\vec{e}_\alpha \cdot \vec{u}}{s^2} + \frac{9}{2}\frac{(\vec{e}_\alpha \cdot \vec{u})^2}{c^4} - \frac{3}{2}\frac{\vec{u} \cdot \vec{u}}{c^2})$
    $g_\alpha^{eq}(\vec{x}, t) = \epsilon \rho w_\alpha (1 + 3\frac{\vec{e}_\alpha \cdot \vec{u}}{s^2} + \frac{9}{2}\frac{(\vec{e}_\alpha \cdot \vec{u})^2}{c^4} - \frac{3}{2}\frac{\vec{u} \cdot \vec{u}}{c^2})$
    $\Delta f_\alpha = -w_\alpha \rho \alpha \epsilon \frac{\vec{e}_\alpha}{|\vec{e}_\alpha|} \cdot \vec{g}$
    $\tau_g = \frac{3\kappa}{S^2 \Delta t} + \frac{1}{2}$
    $\tau_f = \frac{3\nu}{S^2 \Delta t} + \frac{1}{2}$
    $f_\alpha = f_\alpha + \frac{f_\alpha^{eq} - f_\alpha}{\tau_f} + \Delta f_\alpha$
    $g_\alpha = g_\alpha + \frac{g_\alpha^{eq} - g_\alpha}{\tau_g}$
end while

Advection tests

Here I pressent some simple tests that show how accurately my advection scheme is performing in both geometries. Next we tested

the accuarcy of the advection schemes. Thermal diffusivity (κ) and thermal expansion (α) were set to zero to avoid convection. The fluid was set to temperature 0 (arb. units) except a small segment which was set to 1 shown in yellow top left of figure 2, 3, 4, 5. A streamfunction ψ_c was enforced to produce diagonal back and forth motion or a continous horizontal or azimuthal motion to cross a periodic boundary. Details of the streamfunctions used are given in appendix.
The advection results for both codes are similar. For the periodic advection test figures 2 and 4 the temperature 1 region was advected across the periodic boundary without additional distortion. The centroid (red dot) also lagged the advection field by $\approx 1\%$ and $\approx 10\%$ for the cartesian (figure 4) and polar case (figure 2) respectively. It is unknown why these differ substantually, but a probable cause is a smaller timestep used to produce the polar tests. In all cases, the bluring shows numerical diffusion which happens along the direction of the advection field as predicted by equation **??**.

Simulations

The cartesian and polar streamfunction-vorticity codes are limited in two distinct ways. The polar geometry of the 2-dimensional inner core is well suited to polar coorindates. However, by using polar coorindates, a singularity in the governing equations occures at the center $r \to 0$. For standard regularly spaced meshes as is used here, this causes the lattice spacing near the center to become infinicimal requiring small timesteps and large amounts of compute time. For this reason, the inner region of the polar domain is exlcuded leaving out a critical region in the simulation. In cartesian coorindates, there is no singularity and the full domain is included, however it becomes difficult to recreate the polar geometry and enforce boundary conditions. Because of this, we approximate the 2-dimensional inner core by "unrolling" as shown in figure 6, losing the affect of the polar geometry.

How much does the geometry matter

In this section I compaire the results from the polar and cartesian streamfunction-vorticity codes with similar Prantl and Rayleigh number to see how the geometry affects convection.
A gravitational field linearly proportional to height and radius for the cartesian and polar codes respectively was set. A constant internal heating field H was set for all but the upper 10% of both domains. A compensating heating field was set at the remaining top of the domain to balence the total heat generation. Note this heat field is different in the cartesian and polar cases. In all heating fields time-independent random flucations of $\approx 1\%$ were set to faciliate instabilities.
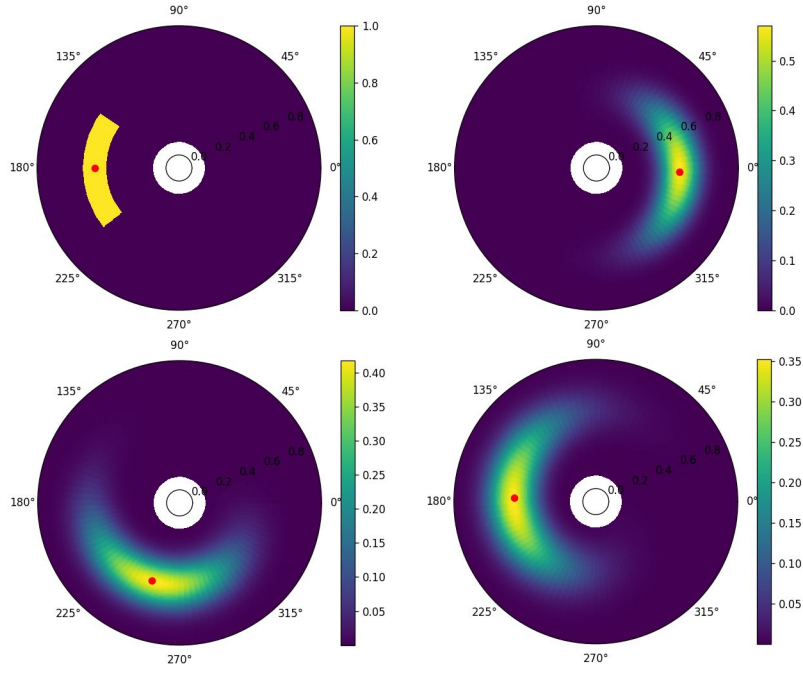
Figure 2: Polar azimuthal advection test. Temperature (color) is plotted in polar space. Red dot indicates temperature weighted mean position within the fluid and is taken as the location of the temperature 1 zone. Fluid is advected by an anticlockwise flow. Cronological order is Top left, top right, bottom left, bottom right. Top left shows the initial condition. Top right shows advection across periodic boundary. Bottom left is state when an exact scheme would have returned to the original position. Bottom right is the final state after being advected around one rotation.
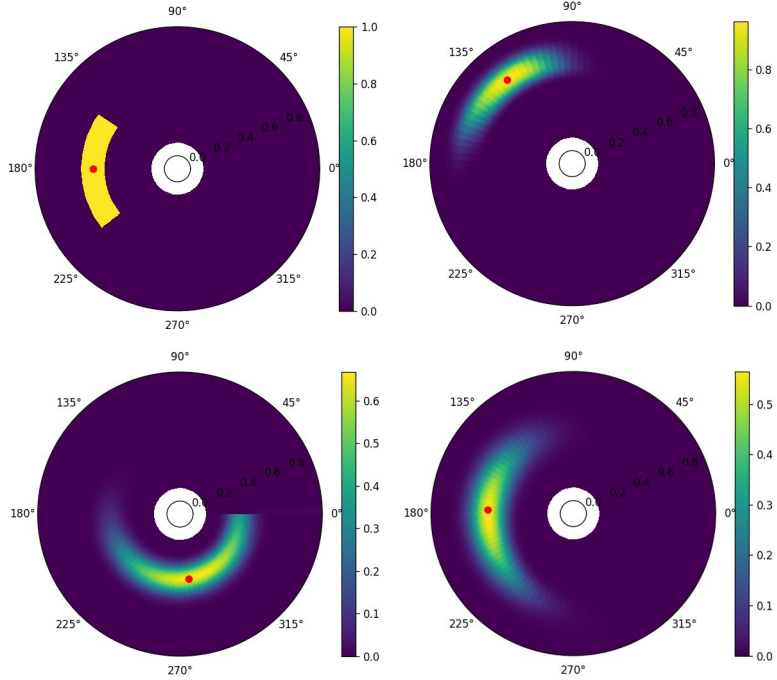

Figure 3: Polar coorindate diagonal advection test. Similar convection used to figure 2. Fluid is diagonally advected over a time t from the initial state (top left) to top right. The advection field is reversed for time $2t$ giving bottom left. The field is reversed again producing bottom right.

How much does the central region matter?

Thermal Lattice Boltzman Simulations

Dicussion

Conclusion

Appendix

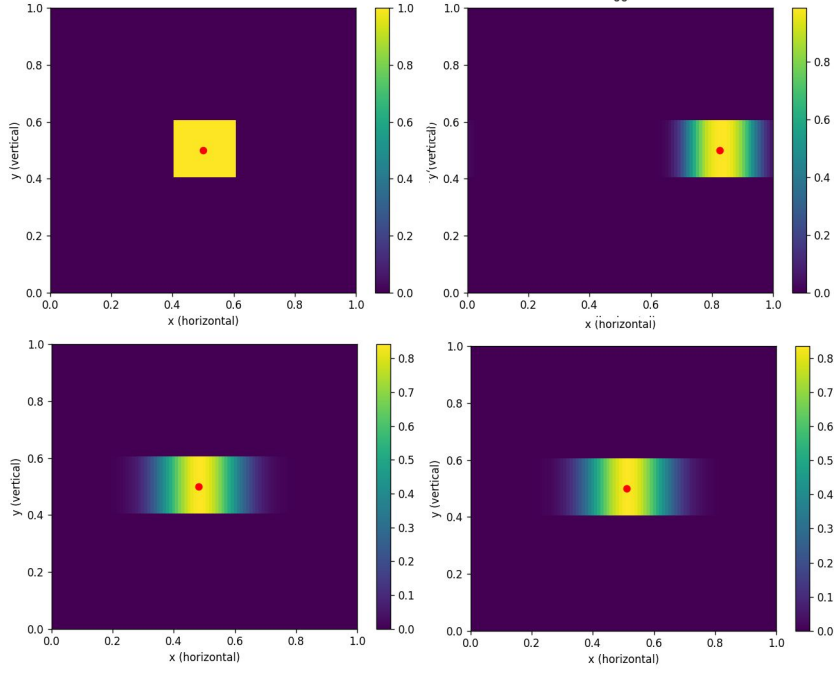## Derivation of Graviational Field in a self gravitating fluid

Figure 4: Cartesian coordinate advection test accross a periodic boundary. Convention similar to figure 2.
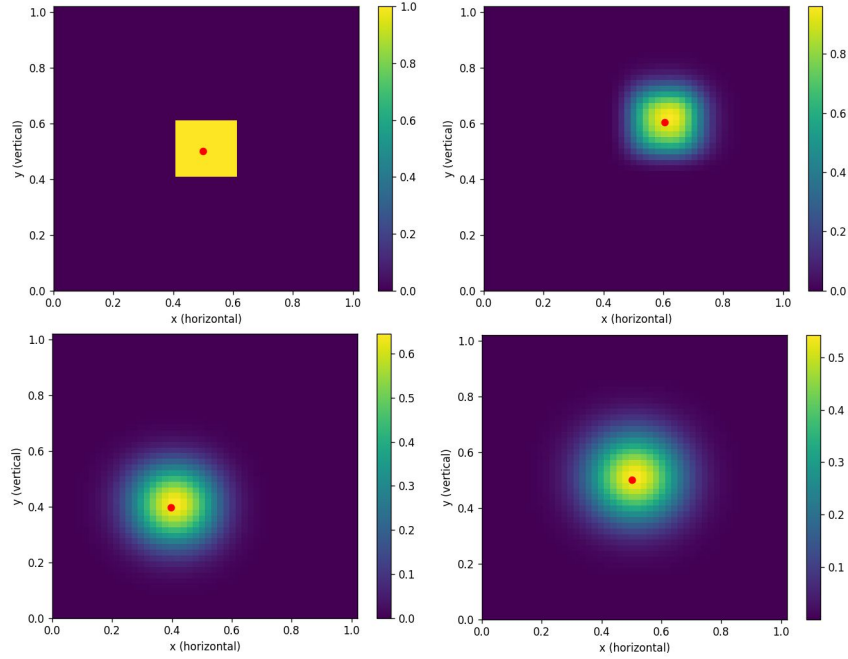

Figure 5: Cartesian diagonal advection test. Similar convention to figure 3.

Some Scales that I used

This is an important source here [1].

We chose the following legnth scales for the problem. For length we used d, the height or radius of the domain, for timescale we used $\frac{d^2}{\kappa}$, for pressure we used $\frac{\rho_0 d^2}{\kappa}$, for temperature we used $\frac{d^2 H}{\kappa}$. I took the rayleigh number as $Ra = \frac{g\alpha H d^5}{\nu\kappa^2}$ and the Prantl number $Pr = \frac{\nu}{\kappa}$. I additionally define a timescale for transport via flow:

$$\tau = \frac{\kappa\nu}{g\alpha H d^3} \tag{33}$$

References

[1] D. Goluskin. *Internally heated convection and Rayleigh-Bénard convection.* Springer, 2016.

shutterstock.com · 1188115291

Figure 6: figure showing how the 2-dimensional polar domain is "unrolled" into a 2-dimensional cartesian domain.

[2] R. Khazaeli, M. Ashrafizaadeh, and S. Mortazavi. A ghost fluid approach for thermal lattice boltzmann method in dealing with heat flux boundary condition in thermal problems with complex geometries. 2015.

[3] P. Mora and D. A. Yuen. Simulation of plume dynamics by the lattice boltzmann method. *Geophysical Journal International*, 210(3):1932–1937, 2017.

shutterstock.com · 1188115291

Figure 7: Internally Heated Convection comparison between cartesian case (left) and polar case (right) $Pr = 1, Ra = 10^8$